KSME

Springer

Journal of Mechanical Science and Technology 37 (10) 2023

Original Article
DOI 10.1007/s12206-022-0806-2

Keywords:
- Photovoltaic power
- Organic solar cell
- Zinc oxide/poly vinyl alcohol thin film
- Solution casting technique
- Energy conversion efficiency

Correspondence to:
Ataur Rahman
arat@iium.edu.my;
Shaheer Ahmed Khan
shaheer.ahmedkhan@yahoo.com

Citation:
Khan, S. A., Rahman, A., Khan, W., Haider, S. M. (2023). Characterization and application of nano-composite zinc oxide /poly vinyl alcohol thin-film in solar cell performance enhancement. Journal of Mechanical Science and Technology 37 (10) (2023) 5055~5065.
http://doi.org/10.1007/s12206-022-0806-2

Received March 10th, 2021
Revised August 14th, 2021
Accepted May 22nd, 2022

† Recommended by Editor Chongdu Cho

Characterization and application of nano-composite zinc oxide/poly vinyl alcohol thin-film in solar cell performance enhancement

Shaheer Ahmed Khan[1,2,3], **Ataur Rahman**[1], **Wajahat Khan**[2] **and Syed Mustafa Haider**[4]

[1]Department of Mechanical Engineering, Faculty of Engineering, International Islamic University Malaysia, 50728 KL, Malaysia, [2]Department of Engineering Sciences, Pakistan Navy Engineering College (PNEC), National University of Sciences and Technology (NUST), Karachi-75350, Pakistan, [3]Department of Materials Engineering, NED University of Engineering and Technology (NEDUET), Karachi -75270, Pakistan, [4]Department of Industrial and Manufacturing Engineering, Pakistan Navy Engineering College (PNEC), National University of Sciences and Technology (NUST), Karachi-75350, Pakistan

Abstract Flexible, economical, and low-toxic organic solar cells are becoming highly popular in photovoltaic research. Interestingly, its efficiency of energy conversion remains lower than that of silicon-based solar cells. As a result, it is unavoidable to focus on organic solar cell efficiency enhancement. This article presents a nano-composite thin-film developed using zinc oxide (ZnO) and polyvinyl alcohol (PVA) with a solution casting technique varying weight percentage (wt.%) of ZnO into the PVA matrix. The characterization of the thin-film of ZnO/PVA has been made using SEM, XRD, FTIR, and UV-Vis spectroscopy. The characterization reveals that the ZnO nanoparticle network forms an excellent path for electron flow in the PVA matrix at the optimal ZnO concentration of 16.66 % and a PVA concentration of 83.33 %. The thin film was applied to an organic solar cell of architecture consists of carbon fiber reinforced with ZnO-epoxy resin/CuO-epoxy resin for performance investigation. The solar cell's maximum efficiency was determined to be 9.01 % before and 14.65 % after using the nanocomposite film. 5.64 % increase in the efficiency of organic solar cells are observed after the ZnO/PVA nanocomposite thin film is applied.

1. Introduction

There has been a rapid increase in the use of a type of renewable energy [1]. Solar cell technologies have developed in many stages of development, for example, the first generation of solar technologies uses inorganic molecules mainly silicon as a medium for the processing of solar energy, the second generation of solar cells used compound semiconductors such as GaAs, CdTe, a-Si, etc., along with the advent of thin film based solar cells utilizing inorganic molecules and the third generation of solar cells employs organic molecules primarily semiconductor polymers as a light absorber for the manufacture of solar cells treated with solution. Third generation solar cells essentially involve the use of nano-crystalline materials which promise both lower production costs and improvement [2].

Nanocomposites have been widely used in the fabrication of third-generation solar cells, namely thin film organic solar cells, with the goal of optimising solar energy harvesting. Numerous researchers have observed improved electrical, optical, thermal, and dielectric properties in PVA nanocomposites based on ZnO prepared in a variety of ways. Numerous physical and chemical methods have been used to develop, produce, and characterise ZnO/PVA nanocomposites, including in situ methods, solution casting, melt processing, and chemical vapour deposition methods [3, 4]. Numerous researchers have investigated the structure, optical, and dielectric properties of PVA doped with ZnO. Kochi et al. [5] observed that the optical energy gap in a doped polymer decreases with increasing doping concentration up to 8 % ZnO. Doping PVA mixtures improves their optical and photoluminescence properties. Hassan et al. [6] demonstrated that a ZnO/PVA nanocomposite has a high absorption, a small energy gap, and average optical conductivity. The energy band difference between ZnO and PVA was determined to be 4.8 eV. The refractive index (n) and dielectric constant are also increased when ZnO dopant nanoparticles are used. Ambrosio et al. [7] observed that the addition of ZnO nanoparticles altered the absorbance near the UV region and that the maximum band gap was 5.83 eV for the sample with a higher ZnO content. Shanshool et al. [8] proposed that low transmittance was inversely proportional to the concentration of ZnO nanoparticles in the UV field. It was discovered that the optical band gap of the nanocomposite is redshifted. For all samples, the energy gap values decreased as the weight percentage of ZnO nanoparticles in the nanocomposite increased. Abdel-Galila et al. [9] investigated the TEM image and confirmed the formation of a ZnO nanoparticle with an average size of 28-52 nm. The XRD patterns revealed the amorphous nature of PVA and the nanostructure of the ZnO/PVA composite. The addition of ZnO nanoparticles increased the thermal stability of the PVA polymer. With increasing ZnO content, the optical bandgap of ZnO/PVA nanocomposites has decreased. According to Hemalatha et al. [10], the average crystal size of ZnO is between 30 and 38 nm. These films exhibit ultraviolet luminescence at room temperature and a reasonable increase in photoluminescent intensity when 10 mol percent is added, indicating their potential use in optoelectronic devices. Due to the variability in crystalline size and aggregate formation, crystallinity increased to 15 % mol percent doping and then decreased to 20 % mol percent doping. According to Viswanath et al. [11], the approximate average crystallite size of XRD is 41 nm. The addition of ZnO nanoparticles enhanced the optical properties of the virgin PVA matrix. A concentrated nanocomposite (3 %wt.) has the highest absorption, the smallest energy gap, and the highest optical conductivity. Both of these advantages enable a broad range of solar cell applications for the ZnO/PVA nanocomposite with a ZnO concentration of 3 wt.%. Aashis et al. [12] determined that the 558 cm^{-1} FTIR peak indicated the presence of ZnO in the composites. The XRD analysis revealed that the crystal structure of the ZnO remained unchanged following the preparation of the composites. Analyze the surface of ZnO/PVA nanocomposite films by observing that the 0.5 wt.% film surface is smoother than the surface of other composite films.

It is evident from the above literature review that these researchers suggested using ZnO/PVA nanocomposite films in solar cells, but to the author's knowledge, no study has been conducted on the incorporation of nanocomposite films in solar cells. The primary goal of this work is to address a research gap in the application of ZnO/PVA nanocomposite film to solar cells. For this reason, this study was conducted. The preparation of Nano-composites thin films with PVA as the polymer matrix and ZnO nanoparticles is discussed in this manuscript. The ZnO/PVA films are prepared using the solution casting method. SEM, FTIR, XRD, and UV-Vis spectroscopy were used to characterize the sample. The objective is to improve the performance of organic solar panels by 3 % to 5 %. The creation of a nanocomposite film ZnO/PVA with varying weight percentages of ZnO and PVA, as well as an examination of its effect on the performance enhancement of organic solar cells [(C-ZnO/epoxy resin)/(CuO/epoxy resin)/carbon fibre] and the observation of changes in solar cell efficiency [14].

Table 1. Physical properties of ZnO [13].

Property	Value
Molecular mass (g/mol)	81.389
Density (g/cm^3)	5.6803
Melting point (°C)	1975
Specific gravity at 300 K (g/cm^3)	5.642
Energy gap (eV)	3.4, direct
Exciton binding energy (meV)	60

1.1 Overview of zinc oxide (ZnO)

Zinc oxide is a naturally occurring inorganic compound with the chemical formula ZnO. It is an n-type semiconductor in the group II-VI region with a large band gap of approximately 3.33 eV. Numerous unique properties of ZnO have been identified, including excitonic emission at or above room temperature, optical transparency in the visible range, a high surface-to-volume ratio, and the quantum containment effect [15]. Chemical bath deposition is particularly well-suited for growing large-area ZnO films with intriguing properties for photoelectron-chemical solar cells [16]. This technique is intended for the fabrication of ZnO nanostructures on a variety of substrates, including glass microscopy and steel. Band-gap engineering can be used to control the conductivity of ZnO [17]. By introducing small amounts of native point defects and impurities (dopants) (down to 14 cm^3 or 0.01 ppm), it is possible to significantly alter the electrical, structural, optical, and morphological properties of semiconductors [18].

According to the above literature, the physical properties of ZnO nanoparticles, such as optical, electrical, and magnetic, significantly increase the solar energy harvesting efficiency of ZnO composite materials. The majority of ZnO's significant physical properties are listed in Table 1.

1.2 Overview of polyvinyl alcohol (PVA)

PVA is a white-colored, non-toxic, semi-crystalline, water soluble and thermostable compound with exceptional optical properties, enormous dielectric properties, and a high capacity for charge storage [19]. PVA decomposes rapidly above 200 °C due to its pyrolysis susceptibility. PVA films superior optical quality makes them ideal for optical sensors and devices [20]. PVA is versatile, solid, and hard, with the ability to act as an oxygen/aroma barrier. Moisture must be avoided at all costs to

Table 2. Physical properties of PVA [21].

Parameters	Description/value
Molecular weight (g/mol)	20000 to 400000
Density (g/cm^3)	1.19-1.31
Melting point (°C)	230 °C
Specific gravity at 300 K (g/cm^3)	1.3
Stability to sunlight	Excellent
Thermal stability	Decomposition at ~200 °C
Solubility	Soluble in water

avoid any PVA disruption of gas permeability. Physical modification of PVA is possible via the crystallization process. PVA crystallizes due to the hydrogen bond between its chains. When exogenous nanoparticles (NPs) are incorporated into a polymer matrix, they act as nucleating agents during crystallization [22]. The physical properties of pure PVA are listed in Table 2.

2. Development of ZnO/PVA nanocomposite film

Sigma-Aldrich supplied the polyvinyl alcohol (PVA) code 363146, which has an average molecular weight (Mw) of 98000 and is 99+ % hydrolyzed. Zinc oxide (ZnO) was purchased from Malaysia-based R & M Chemicals. It was used as a filler in nanocomposites of polymers and zinc oxide. The nanoparticles had a diameter of 100 nm (nanometers of 10 x 10^{-3} mm). Deionized water (H_2O) was used as a solvent for PVA because it has no charge (is ion-free and does not conduct electricity). It is frequently used as a solvent for this type of polymer. It is a polar protic solvent with a long hydrocarbon chain structure.

2.1 Solution casting method

The solution casting method (SCM) is a simple and economical technique for fabricating nanocomposite thin films on a laboratory scale. The SCM is used in this study to fabricate thin films of ZnO/PVA nanocomposites on a laboratory scale. A glass template (petri dish) with the required shape (lab scale) of the nano-composite thin film was developed for this study in order to investigate its composition and perform experiments with organic solar cells to validate it. The liquid nanomaterial composition contains ZnO, PVA, and deionized water in the proportions specified (H_2O). The resulting liquid was agitated in an ultrasonic bath for 30 minutes before being poured into a template. It is then allowed to harden for 48 hours in a forced convection oven set to 60 °C. Consequently, the solidified nanocomposite thin film was formed, and the template was removed. This thin film is both rigid and flexible, allowing it to be fitted to solar cells of any shape.

2.2 Preparation of polymer alcohol-ZnO nanocomposite

To prepare ZnO/PVA Nano-composites, PVA was used as the polymer matrix and ZnO nanoparticles were used as fillers. The different weight percentage (wt.%) of ZnO and PVA was dissolved in distilled water and prepared a sample for the thin film using the solution casting technique as shown in Fig. 1. The weight percentage of ZnO in the nano-composite (wt %) was calculated based on the equation,

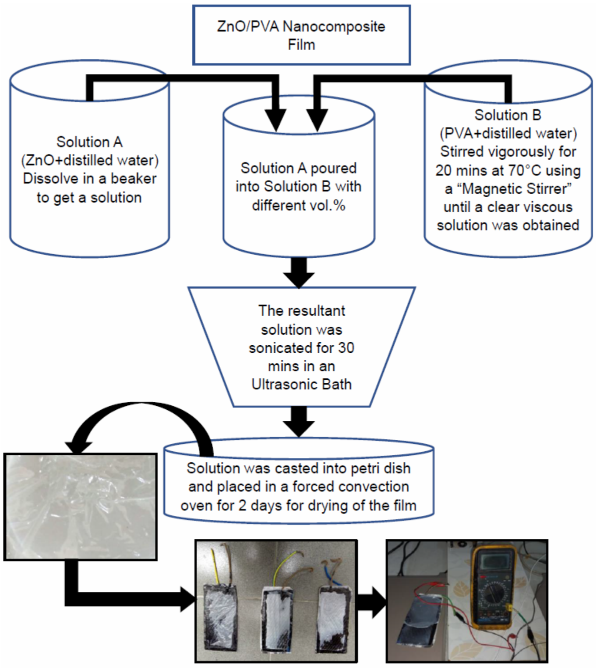

Fig. 1. Flowchart of preparing ZnO/PVA Nano-composite via solution casting.

$$W_f\left(wt.\%\right)=\frac{W_f}{W_P+W_f}\times100\% \qquad (1)$$

where w_t% is the weight percentage of ZnO in the nanocomposite, W_p is the weight of the polymer and W_f is the weight of the filler.

3. Characterization

The characterization of ZnO/PVA thin film has been made with scanning electron microscope (SEM) for the morphological analysis of the nanocomposite film, Fourier transform infrared spectroscopy (FTIR) for the observation of the presence of functional groups present in nano composite film, X-ray diffraction (XRD) for the examination of the diffraction pattern of the nanocomposite film, UV-visible spectrophotometer (UV-Vis) to investigate the absorption and bandgap of nanocomposite film.

3.1 Scanning electron microscope (SEM)

Fig. 2 shows the SEM machine used for characterization of the ZnO/PVA nano-composite structure. Fig. 3(a) shows the formation of nano-sized crystal aggregates as a result of the high surface energy. There are several small particles averaging less than 14 nm in diameter when dispersed in the PVA and it could be supported by the authors [23].

The aggregate shape causes a non-linear electron flow, which leads to a decrease in energy generation, and it is supported by the conclusion of the authors [24]. Fig. 3(b) demonstrates that the nanoparticles are distributed uniformly within the PVA matrix. The ZnO / PVA nanocomposite demonstrated that crystallites formed and began to grow in the immediate vicinity of the surface as the ZnO concentration was increased. Additionally, it demonstrated uniform dispersion of ZnO nanoparticles, whereas increased ZnO concentration resulted in increased compactness and aggregation and it is supported by the authors [25]. Fig. 3(c) examines the nanoparticles' uniform dispersion within the PVA matrix. The analysis of the surface morphology of the ZnO/PVA composite film shows several aggregates or chunks dispersed randomly on the film's surface. It is critical to note that irregular ZnO nanoparticles ranging in size from 15 to 18 nm were formed. Fig. 3(d) shows a smooth PVA matrix with chunks of flaked shaped ZnO particles scattered around the surface. It is significant to mention that irregular ZnO nanoparticles with diameters ranging from 16 to 19 nm were formed. Fig. 3(e) shows a micrograph of the ZnO/PVA film with a higher PVA concentration in the matrix, arising from inappropriate ZnO mixing.

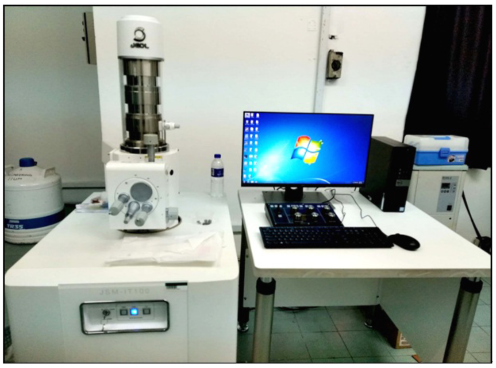

Fig. 2. Scanning electron microscope (JSM-IT100 model).

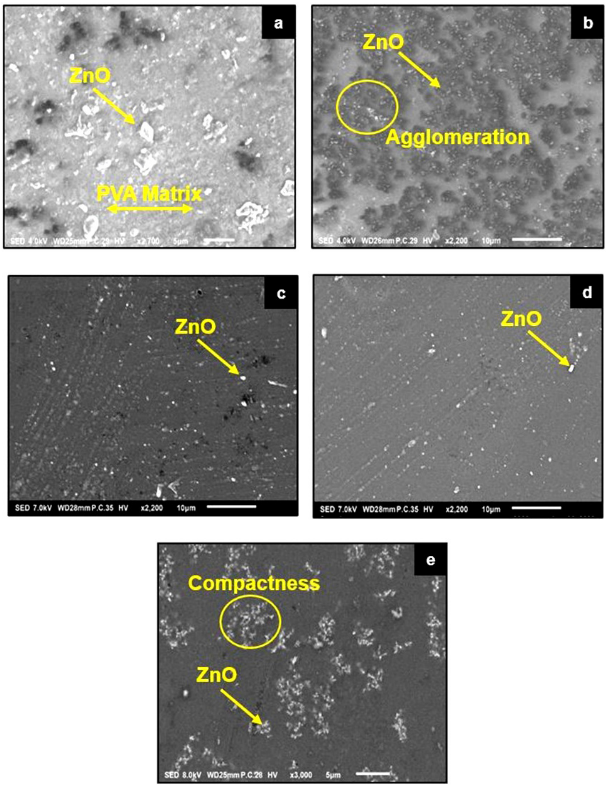

Fig. 3. SEM image: (a) wt.% ZnO 16.66 and wt.% PVA 83.33; (b) wt.% ZnO 28.57 and wt.% PVA 71.42; (c) wt.% ZnO 37.50 and wt.% PVA 62.50; (d) wt.% ZnO 50 and wt.% PVA 50; (e) wt.% ZnO 40 and wt.% PVA 60.

3.2 Fourier-transform infrared spectroscopy (FTIR)

Fourier transform infrared (FTIR) spectroscopy of the synthesized ZnO/PVA film was performed to identify the functional groups present in the film and to analyze the interaction between cross-linked PVA and ZnO nano-particles. The as-prepared samples were checked by using Fourier transform infrared (FTIR) spectroscopy (brand: Perkin Elmer, range: 4000 cm^{-1}-400 cm^{-1}) as shown Fig. 4. The FTIR spectra were caused by the transmittance mode. All spectra were recorded and analyzed. The results of FTIR were used to complement those of the SEM results. The associated functional groups (C-H, CH_2, and C-O) are shown in Table 3 along with their infrared band positions. Additionally, the spectra reveal a broad absorption peak for the PVA/ZnO nanocomposite at higher infrared

Table 3. FTIR infrared band positions.

Figure	C-H	CH_2	C-O
(a)	2907	1415, 1326	1083
(b)	2907	1416, 1327	1086
(c)	2908	1415, 1325	1087
(d)	2912	1414, 1326	1086
(e)	2909	1416, 1325	1085

Fig. 4. Fourier transform infrared (FTIR) spectrometer.

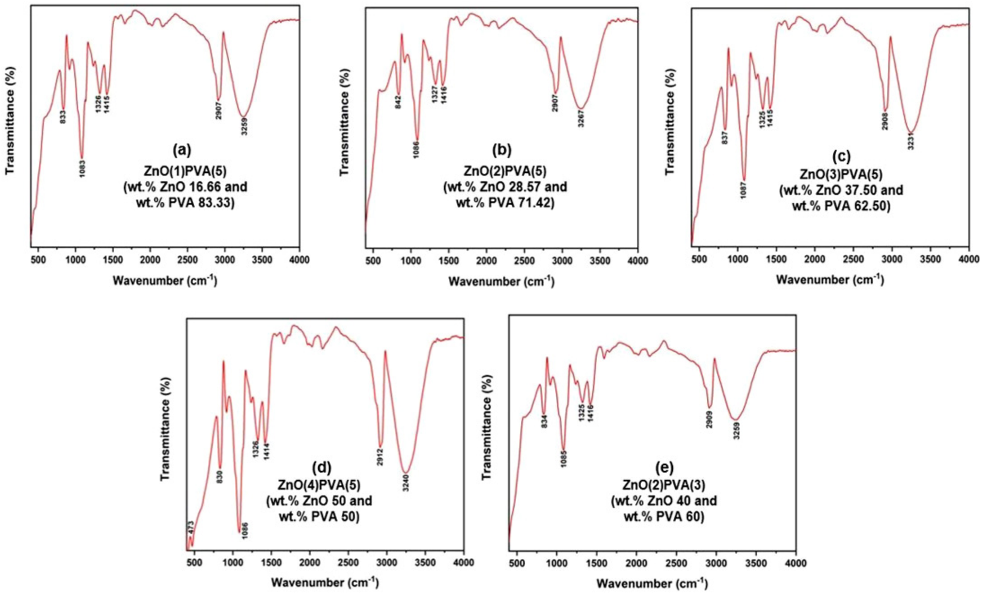

Fig. 5. FTIR spectra of 5 different samples of ZnO/PVA nanocomposite films.

bands as shown in Fig. 5. C-H vibrates asymmetrically. The absorbance is related to the vibrations of CH_2. The PVA matrix acetyl group undergoes C-O stretching [26]. The spectral shift could be due to the formation of intermolecular hydrogen bonds between the OH group of PVA and the ZnO surface. The shift in the associated doping bands indicates that PVA and ZnO interact. The band corresponds to the C-O stretching on the PVA matrix of the acetyl groups present. The change in the respective doping bands shows that PVA and ZnO interact.

3.3 X-ray diffraction (XRD)

An X-ray diffraction (XRD) pattern was used to obtain the structural properties of different ZnO/PVA nanocomposite samples were recorded by the Bruker D2 Phaser 2nd Generation using Cu Kα radiation at a wavelength of 1.54 Å as shown in Fig. 6. The scanning was done in the range of 2 θ values between 20° to 80° at a scan rate of 2 degrees/min. The crystallite size for nanocomposite samples has been measured by using the Scherrer equation below:

$$D = \frac{K\lambda}{\beta COS\theta} \tag{2}$$

where, K = 0.89 (shape factor), λ = 1.5406 Å (wavelength of copper Kα), β = full width at half maximum (FWHM) (radians), and θ = peak position.

Fig. 7(a) illustrates the XRD pattern of the nanocomposite film, which exhibits a relatively high peak of 2 θ = 35.96. These diffraction peaks confirm the formation of a ZnO/PVA nanocomposite. The crystallite size of PVA/ZnO nanocomposite films was determined using the Debye Scherrer formula and was found to be between 14.19 and 14.28 nm, while the average particle size (D) is approximately 14.23 nm.

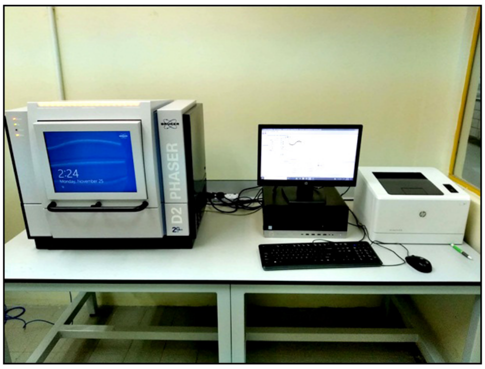

Fig. 6. X-ray diffraction.

Fig. 7(b) illustrates the XRD pattern of the nanocomposite film exhibits a relatively high peak at 2 θ = 35.64. These diffraction peaks confirm the formation of a ZnO/PVA nanocomposite. Due to the variability in crystalline size and aggregate formation, doping ZnO nanoparticles results in an increase in crystallinity. The crystallite size of PVA / ZnO nanocomposite films was determined using the Debye Scherrer formula and was found to be in the range of 16.37-17.84 nm, while the average particle size (D) is approximately 17 nm. Fig. 7(c) illustrates the XRD pattern of the nanocomposite film exhibits a relatively high peak of 2 θ = 36.39. These diffraction peaks confirm the formation of a ZnO/PVA nanocomposite. Due to the variability in crystalline size and aggregate formation, doping ZnO nanoparticles results in an increase in crystallinity. The crystallite size of PVA/ZnO nanocomposite films was determined using the Debye Scherrer formula and was found to be in the range of 15.54-18.79 nm, while the average particle size (D) is approximately 17 nm. Fig. 7(d) illustrates the XRD pattern of the nano composite film that exhibits a relatively high peak of 2 θ = 36.37. These diffraction peaks confirm the formation of a ZnO/PVA nanocomposite. Excessive doping of ZnO nanoparticles reduces crystallinity due to crystalline size variability and aggregate formation. The crystallite size of PVA/ZnO nanocomposite films was determined using the Debye Scherrer formula and was found to be in the range of 16.86-19.55 nm, while the average particle size (D) is approximately 18.31 nm. Fig. 7(e) illustrates the XRD pattern of the nanocomposite film exhibits a relatively high peak of 2 θ = 36.78. Except for Fig. 7, all of the associated diffraction peaks correspond to the PVA diffraction peak and the regular ZnO wurtzite hexagonal crystal struc ture PDF database (JCPDS 36-1451) [27].

3.4 Ultraviolet-visible spectrophotometer (UV-Vis)

The ultraviolet-visible spectrophotometer (UV-Vis) (Fig. 10) was carried out to test the samples of ZnO/PVA nanocomposite in order to find the absorption spectrum and energy bandgap. For the experiment, the equipment was first calibrated, and the samples were placed in the chamber which is parallel to the UV visible source so that the rays of a known wavelength passed through the deposited layer on the substrate of the sample. The energy bandgap, absorption spectrum and the effect of zinc oxide nanoparticles on the PVA matrix were obtained.

Fig. 8(a), the absorption spectrum of the nano composite film,

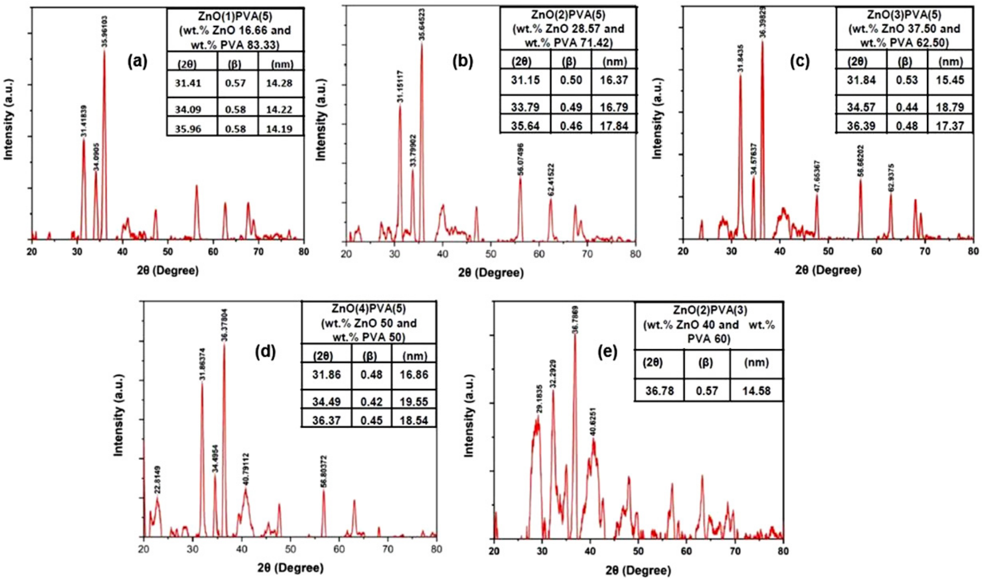

ZnO(1)PVA(5) (wt.% ZnO 16.66 and wt.% PVA 83.33)

(2θ)	(β)	(nm)
31.41	0.57	14.28
34.09	0.58	14.22
35.96	0.58	14.19

ZnO(2)PVA(5) (wt.% ZnO 28.57 and wt.% PVA 71.42)

(2θ)	(β)	(nm)
31.15	0.50	16.37
33.79	0.49	16.79
35.64	0.46	17.84

ZnO(3)PVA(5) (wt.% ZnO 37.50 and wt.% PVA 62.50)

(2θ)	(β)	(nm)
31.84	0.53	15.45
34.57	0.44	18.79
36.39	0.48	17.37

ZnO(4)PVA(5) (wt.% ZnO 50 and wt.% PVA 50)

(2θ)	(β)	(nm)
31.86	0.48	16.86
34.49	0.42	19.55
36.37	0.45	18.54

ZnO(2)PVA(3) (wt.% ZnO 40 and wt.% PVA 60)

(2θ)	(β)	(nm)
36.78	0.57	14.58

Fig. 7. XRD patterns of 5 different samples of ZnO/PVA nanocomposite films.

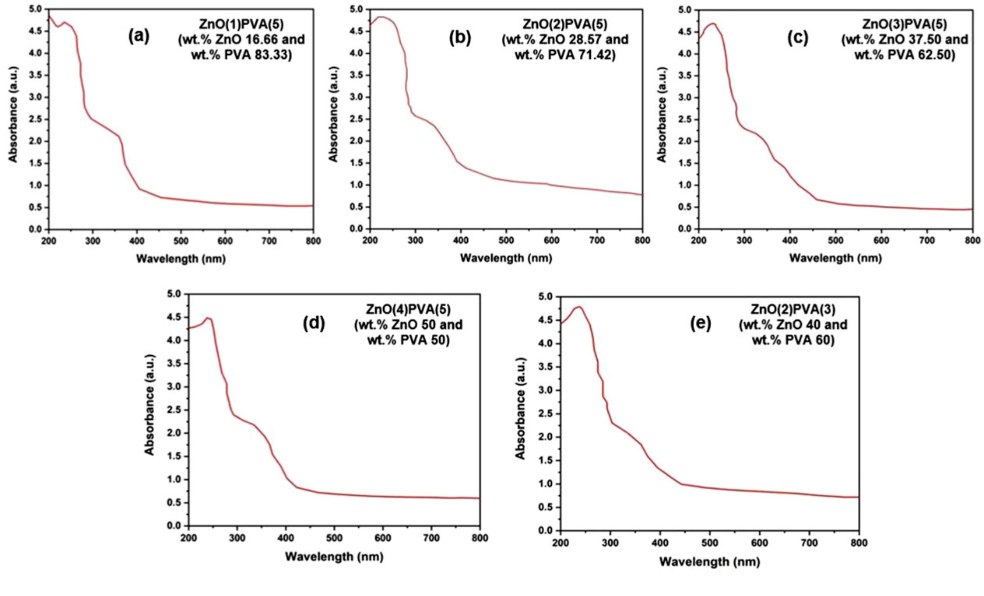

Fig. 8. Absorbance of 5 different samples of ZnO/PVA nanocomposite films.

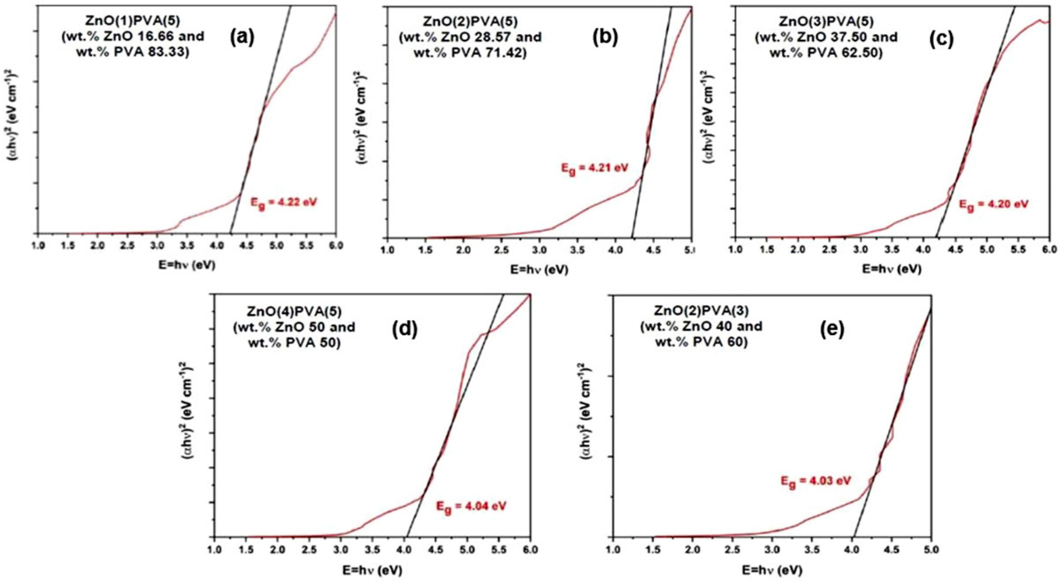

Fig. 9. Optical band gap energy of 5 different samples of ZnO/PVA nanocomposite films.

demonstrates two bands at 235 nm and 356 nm with a lower intensity, indicating the presence of ZnO in the film [28]. These bands are attributed to the absorption of PVA and the excitons of ZnO nanoparticles. By converting the spectrum to Tauc's plot, the energy bandgap is determined to be 4.22 eV as shown in Fig. 9(a). Fig. 8(b), the absorption spectrum of the ZnO/PVA composite film, demonstrates two bands at 225 nm and 340 nm with a lower intensity, indicating the presence of ZnO in the film. These bands are attributed to the absorption of PVA and the excitons of ZnO nanoparticles. By converting the spectrum to Tauc's plot, the energy bandgap is determined to be 4.21 eV as shown in Fig. 9(b). Fig. 8(c), the absorption spectrum of the ZnO/PVA composite film, demonstrates two bands at 234 nm and 335 nm with a lower intensity, indicating the presence of ZnO in the film. These bands are attributed to the absorption of PVA and the excitons of ZnO nanoparticles. By converting the spectrum to Tauc's plot, the energy bandgap is determined to be 4.20 eV as shown in Fig. 9(c). Fig. 8(d), the absorption spectrum of the ZnO/PVA composite film, demonstrates two bands at 239 nm and 339 nm with a lower intensity, indicating the presence of ZnO in the film. These bands are attributed to the absorption of PVA and the excitons of ZnO nanoparticles. By converting the spectrum to Tauc's plot, the energy bandgap is determined to be 4.04 eV as shown in Fig. 9(d). Fig. 8(e), the absorption spectrum of the ZnO/PVA composite film, demonstrates two bands at 238 nm and 356 nm with a lower intensity, indicating the presence of ZnO in the film. These bands are attributed to the absorption of PVA and the excitons of ZnO nanoparticles. By converting the spectrum to Tauc's plot, the energy bandgap is determined to be 4.03 eV as shown in Fig. 9(e). It is concluded that as the concentration of ZnO nanoparticles in the polymer matrix increases, the absorption edge moves toward the higher wavelength or lower energy associated with the blue/green region of the visible spectrum. Increased nano ZnO concentration in the matrix results in a decrease in the optical energy bandgap.

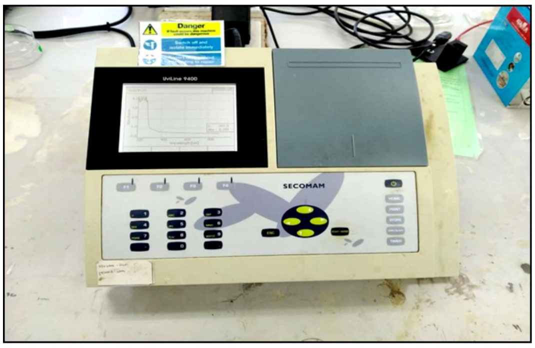

Fig. 10. Ultraviolet-visible spectrophotometer.

3.5 Summary of characterization results

As shown in Fig. 11, the SEM analysis indicates that adding ZnO nanoparticles to the PVA matrix increased agglomeration/aggregation in the ZnO/PVA nanocomposite. This is because the high surface energy results in the formation of clusters at various points on the surface. The XRD results indicate that the degree of crystallinity increases with increasing ZnO concentrations in the matrix and decreases with decreasing ZnO concentrations. UV-Vis results indicate that as the ZnO concentration in the matrix increases, the energy bandgap decreases.

4. Performance investigation of ZnO/PVA solar film

The organic solar has been developed using carbon zinc

Table 4. Performance of the Zn0/PVA samples.

PV cell with ZnO/PVA thin film	Solar temperature 32 °C at 1 PM Malaysia				
	V_{oc} (mV)	J_{sc} (mA/cm^2)	FF (%)	H (%)	Eg (eV)
ZnO (1) PVA (5)	647.33	30.78	73.53	14.65	4.22
ZnO (2) PVA (5)	662.81	31.46	61.99	12.9	4.21
ZnO (3) PVA (5)	637.27	26.61	69.09	11.71	4.20
ZnO (5) PVA (5)	606.31	19.53	64.03	7.58	4.04
ZnO (2) PVA (3)	551.09	22.29	58.29	7.16	4.03

Table 5. Organic solar cell performance with the thin-film of nanocomposite of ZnO (16.66 wt.%)/PVA (83.33 wt.%).

PV cell with ZnO/PVA thin film	V_{oc} (mV)	J_{sc} (mA/cm^2)	Fill factor (FF) (%)	Efficiency (η) (%)
	Without film			
Cell with 70 gsm paper as dielectric	570.88	24.6	64.22	9.01
	With thin film of ZnO (16.66 wt.%)/PVA (83.33 wt.%)			
	647.33	30.78	73.53	14.65

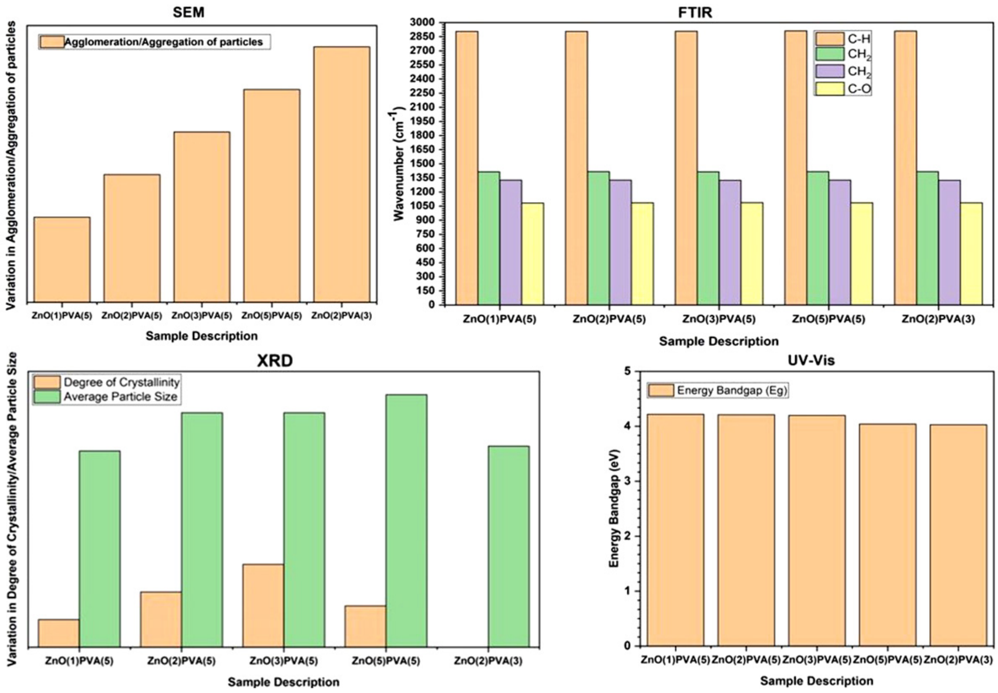

Fig. 11. Summary of characterization results.

oxide (C-ZnO) and copper oxide (CuO) conductive polymer and aqueous dielectric, and reinforced by carbon fibre (CF). The CF fabrics derived from π-carbon (240 g/m^2) 0.25 mm thick were used for the development of organic cells. The CF electrodes were reinforced with nano ZnO (size 10 nm) epoxy for the negative electrode in order to facilitate high electron mobility as a form of n-type semiconductor by adding 5 % of π-carbon (9240 g/m^2) for a band-gap energy of 3.5 eV. Meanwhile, epoxfilled nano-CuO (size 50 nm, Sigma Aldrich) to the positive electrode in order to facilitate bore/positive charging as a p-type semiconductor. Fig. 12 shows the model of aqueous electrolyte sandwiched by C-ZnO/CuO-ER_CFR organic solar cell.

Table 4 illustrates the data of organic solar cells [carbon fibre reinforced with (ZnO/epoxy resin)/(CuO/epoxy resin)] incorporated with ZnO/PVA nano-composite films as well as the results of individual tests of each ZnO/PVA nano-composite sample, all of which were done under direct sunlight. The highest efficiency achieved by ZnO(1)PVA(5) (wt.%: ZnO 16.66 and wt.% of PVA 83.33) is 14.65 % while the lowest efficiency achieved by ZnO(2)PVA(3) (wt.% of ZnO 40 and wt.% of PVA 60) is found to be 7.16 %.

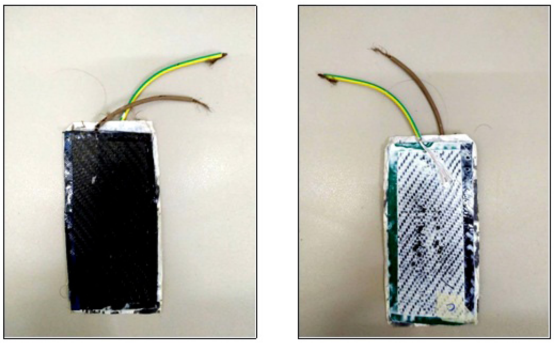

Fig. 12. Laboratory scale organic solar panel with ZnO/pvPVA thin film.

The performance of ZnO/PVA thin film with organic solar cells under a solar heat of 32 °C is shown in Fig. 13, which is based on the J-V characteristics curve. The objective of other thin films of ZnO/PVA is to compare the performance of the

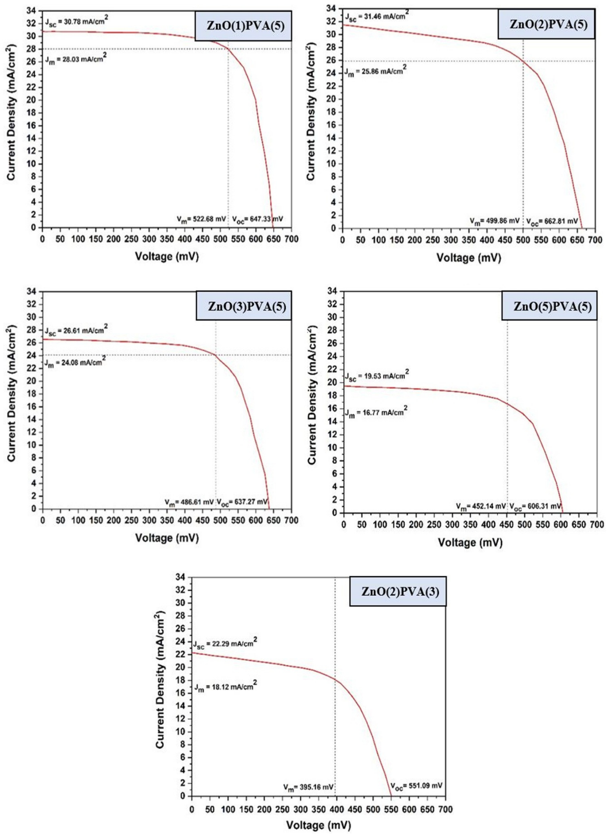

Fig. 13. Performance of 5-samples with organic solar cells.

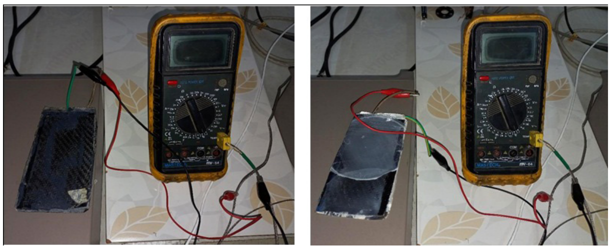

(a) (b)

Fig. 14. Performance of organic solar cell: (a) without ZnO/PVA thin film; (b) with ZnO/PVA thin film.

best (optimized) sample. The performance of other ZnO/PVA samples demonstrates that increasing the weight percentage of the ZnO nanoparticle causes a decrease in organic solar performance enhancement.

This could also lead to a decrease in the band gap of the sample. The low current density indicates that a higher percentage of ZnO forms a wire-film that prevents current carriers from moving freely, resulting in a lower energy development. The summary of the performance of the thin films of ZnO/PVA of various compositions is presented in Table 4. ZnO(1)PVA(5) has the highest efficiency of 14.65 %, while ZnO(2)PVA(3) has the lowest efficiency of 7.16 %. The efficiency of a solar cell decreases as the fill factor of the cell decreases. The optical direct bandgap narrowed as the concentration of ZnO in the polymer matrix increased, resulting in a loss of efficiency.

The ZnO/PVA solar thin film has been prepared with the best (optimized) sample, which has been made with ZnO wt.% of 16.66 and PVA wt.% of 83.33 and tested with the C-ZnO/CuO-ER_CFR organic solar cell. The results of the organic solar cell performance have been measured without and with ZnO/PVA thin film as shown in Fig. 14. The solar cell performance increased from 9.01 to 14.65 %. Table 5 displays the aggregated results.

5. Conclusions

Based on the contents of this manuscript, the following conclusions have been reached:

- ZnO/PVA nano-composites were successfully prepared by the solution casting method. To identify the best sample for modeling the ZnO/PVA thin film, 5 samples were prepared from a blended mixture of ZnO nano powder and PVA matrix with different weight percentages.
- Each sample is then characterized using SEM, FTIR, XRD and UV-Vis machines. Adding ZnO nano-particles to the PVA matrix increased agglomeration/aggregation in the ZnO/PVA nanocomposite. This is because the high surface energy results in the formation of clusters at various points on the surface. The degree of crystallinity increases with increasing ZnO concentrations in the matrix and decreases with decreasing ZnO concentrations. As the ZnO concentration in the matrix increases, the energy bandgap decreases. The optimized samples were then selected based on the results of energy bandgap, V_{oc}, J_{sc}, and η and were found to be ZnO (wt.% of 16.66) and PVA (wt.% of 83.33).
- The solar cell's maximum efficiency before and after using the best nanocomposite ZnO/PVA sample film. The efficiency of energy conversion (η) was determined to be 9.01 % and 14.65 %, respectively. The increase in efficiency of the organic solar cell demonstrated that the ZnO/PVA nanocomposite film has significant potential for use in enhancing the efficiency of organic solar cells.

Acknowledgments

This work is supported by Flagship Project Program “Solar & Wind Power Ultrafast DC-DC Charging Station for Electric Vehicle”, Office of Strategy and Institutional Change (OSIC), International Islamic University Malaysia.

Nomenclature

θ : Peak position, degree
λ : Wavelength, nm
β : Full width at half maximum, radian
η : Solar energy conversion efficiency, %
c : Activated carbon
D : Crystallite size

J_{sc} : Short circuit current density, A/cm^2
V_{oc} : Open circuit voltage, V
w_f : Weight of filler
w_p : Weight of polymer
FF : Fill factor, %
ZnO : Zinc oxide nano-powder
PVA : Poly vinyl alcohol
wt% : Weight percentage, %

References

[1] S. A. Khan and A. Rahman, Efficiency of thin film photovoltaic paint: a brief review, *Int. J. Recent Technol. Eng.*, 7 (2019) 163-169.

[2] G. Tessema Mola, X. G. Mbuyise, S. O. Oseni, W. M. Dlamini, P. Tonui, E. A. A. Arbab, K. Kaviyarasu and M. Maaza, Nanocomposite for solar energy application, *Nano Hybrids and Composites*, 20 (2018) 90-107.

[3] A. Rahman and G. Kibria, Energy storage Al-ZnO/CuO_CFRP organic structural auxiliary power system for electric vehicle, *Solid State Technology*, 26 (1 & 2) (2020) 124-131.

[4] R. Bouzerara, S. Achour, N. Tabet and S. Zerkout, Synthesis and characterisation of ZnO/PVA composite nanofibres by electrospinning, *International Journal of Nanoparticles*, 4 (1) (2011) 10-19.

[5] R. Kochi, V. Crasta, R. Kumar and G. Shetty, Study of structural, optical and photoluminescence properties of ZnO doped PVA/PVP nanocomposite, *AIP Conference Proceedings*, 2100 (1) (2019) 0200452019.

[6] N. J. Mohammed, Z. S. Rasheed and A. S. Hassan, Improvement optical properties of PVA/TiO$_2$ and PVA/ZnO nanocomposites, *Al-Mustansiriyah Journal of Science*, 29 (3) (2019) 118-123.

[7] R. Ambrosio, A. Carrillo, M. L. Mota, K. De La Torre, R. Torrealba, M. Moreno, H. Vazquez, J. Flores and I. Vivaldo, Polymeric nanocomposites membranes with high permittivity based on PVA-ZnO nanoparticles for potential applications in flexible electronics, *Polymers*, 10 (12) (2018) 1370.

[8] H. M. Shanshool, M. Yahaya, W. M. M. Yunus and I. Y. Abdullah, Investigation of energy band gap in polymer/ZnO nanocomposites, *Journal of Materials Science: Materials in Electronics*, 27 (9) (2016) 9804-9811.

[9] A. Abdel-Galila, H. E. Alib and M. R. Balboula, Nano-ZnO doping induced changes in structure, mechanical and optical properties of PVA films, *Arab Journal of Nuclear Science and Applications*, 48 (2) (2015) 77-89.

[10] K. S. Hemalatha, K. Rukmani, N. Suriyamurthy and B. M. Nagabhushana, Synthesis, characterization and optical properties of hybrid PVA-ZnO nanocomposite: a composition dependent study, *Materials Research Bulletin*, 51 (2014) 438-446.

[11] V. Viswanath, S. S. Nair, G. Subodh and C. I. Muneera, Zinc oxide encapsulated poly (vinyl alcohol) nanocomposite films as an efficient third-order nonlinear optical material: structure, microstructure, emission and intense low threshold optical limiting properties, *Materials Research Bulletin*, 112 (2019) 281-291.

[12] R. S. Aashis, S. Gupta, S. Sindhu, A. Parveen and P. C. Ramamurthy, Dielectric properties of novel PVA/ZnO hybrid nanocomposite films, *Composites Part B: Engineering*, 47 (2013) 314-319.

[13] S. J. Pearton, D. P. Norton, K. Ip, Y. W. Heo and T. Steiner, Retracted: recent progress in processing and properties of ZnO, *Progress in Materials Science*, 50 (3) (2005) 293-340.

[14] A. Rahman, K. M. Aung and S. A. Khan, Organic photoelectric-supercapacitor power source of electric vehicle, *Engineering and Management*, 82 (2020) 15175-15182.

[15] M. D. Tyona, R. U. Osuji, F. I. Ezema, S. B. Jambure and C. D. Lokhande, Enhanced photoelectrochemical solar cells based on natural dye-sensitized Al-doped zinc oxide electrodes, *Advances in Applied Science Research*, 7 (2016) 18-31.

[16] P. Jongnavakit, P. Amornpitoksuk, S. Suwanboon and T. Ratana, Surface and photocatalytic properties of ZnO thin film prepared by sol-gel method, *Thin Solid Films*, 520 (17) (2012) 5561-5567.

[17] N. J. Mohammed, Z. S. Rasheed and A. S. Hassan, Improvement optical properties of PVA/TiO$_2$ and PVA/ZNO nanocomposites, *Al-Mustansiriyah Journal of Science*, 29 (3) (2019) 118-123.

[18] G. Machado, D. N. Guerra, D. Leinen, J. R. Ramos-Barrado, R. E. Marotti and E. A. Dalchiele, Indium doped zinc oxide thin films obtained by electrodeposition, *Thin Solid Films*, 490 (2) (2005) 124-131.

[19] W. Z. Abdullah, Y. Dong, I. J. Davies and S. Barbhuiya, PVA, PVA blends, and their nanocomposites for biodegradable packaging application, *Polymer-Plastics Technology and Engineering*, 56 (12) (2017) 1307-1344.

[20] N. Mahanta and S. Valiyaveettil, Surface modified electrospun poly (vinyl alcohol) membranes for extracting nanoparticles from water, *Nanoscale*, 3 (11) (2011) 4625-4631.

[21] M. Aslam, M. A. Kalyar and Z. A. Raza, Polyvinyl alcohol: a review of research status and use of polyvinyl alcohol based nanocomposites, *Polymer Engineering and Science*, 58 (12) (2018) 2119-2132.

[22] Z. Peng, L. X. Kong, S.-D. Li and P. Spiridonov, Poly (vinyl alcohol)/silica nanocomposites: morphology and thermal degradation kinetics, *Journal of Nanoscience and Nanotechnology*, 6 (12) (2006) 3934-3938.

[23] N. B. Kumar, V. Crasta and B. M. Praveen, Advancement in microstructural, optical, and mechanical properties of PVA (Mowiol 10-98) doped by ZnO nanoparticles, *Physics Research International*, 2014 (2014) 742378.

[24] A. F. Mansour, S. F. Mansour and M. A. Abdo, Improvement structural and optical properties of ZnO/PVA nanocomposites, *IOSR Journal of Applied Physics*, 7 (2) (2015) 60-69.

[25] R. Kandulna and R. B. Choudhary, Concentration-dependent behaviors of ZnO-reinforced PVA–ZnO nanocomposites as electron transport materials for OLED application, *Polymer Bulletin*, 75 (7) (2018) 3089-3107.

[26] D. Kumar, S. K. Jat, P. K. Khanna, N. Vijayan and B. Shaibal, Synthesis, characterization, and studies of PVA/co-doped ZnO nanocomposite films, *International Journal of Green Nanotechnology*, 4 (3) (2012) 408-416.

[27] D. M. Fernandes, A. A. Winkler Hechenleitner, S. M. Lima, L.

H. C. Andrade, A. R. L. Caires and E. A. Gómez Pineda, Preparation, characterization, and photoluminescence study of PVA/ZnO nanocomposite films, *Materials Chemistry and Physics*, 128 (3) (2011) 371-376.

[28] O. M. Sabara, J. S. Dunne, A. Q. H. Pedro, J. Trifunović, O. Kotlicic, A. Serrano and I. Kertész, Spectroscopic studies of naproxen and tryptophan immobilized in polyvinyl alcohol, *Biotechnology and Food Science*, 75 (1) (2011) 39-49.

Shaheer Ahmed Khan obtained the bachelor of Engineering in Materials Engineering from the NED University of Engineering and Technology (NEDUET), Pakistan, in 2016. He obtained a research-based master of science degree in Mechanical Engineering from International Islamic University Malaysia (IIUM) in 2021. Currently, he is working as a teaching faculty member at the Pakistan Navy Engineering College (PNEC), National University of Sciences and Technology (NUST), Pakistan, since 2021. Moreover, he is also a Research Scholar at the NED University of Engineering and Technology (NEDUET). His research interests are Materials and Manufacturing Processes, Renewable Energy, and Nanomaterials.

Md. Ataur Rahman obtained the Bachelor of Science (Mechanical Engineering) from the Chittagong University of Engineering and Technology (CUET), Bangladesh in 1991. He has obtained the master of Business Administration (Techno-Entrepreneurship) from the University Technology Malaysia (UTM) in 2000, Master of Engineering (Automotive) from UTM in 2001 and degree of doctor of philosophy in Engineering (Automotive Engineering) from the University Putra Malaysia (UPM) in 2005. He was appointed as a Visiting Fellow for “Designing Automation System for Off-road Vehicle” at the Mechanical Engineering Laboratory, The University of Tokyo, Japan for 2005-2006. He was appointed as an Assistant Professor at the Department of Mechanical Engineering, International Islamic University Malaysia (IIUM) in 2006. Later he was promoted by IIUM for the post of Associate Professor in 2010 and Professor in 2014. He is the Chairmen of IIUM Centre for Excellent of Electric Mobility. His research interests are green transportation system: EV/HEV, intelligent evaporative thermal management system for EV battery, intelligent power train for hybrid and electrical vehicle, intelligent steering system, and traction control system, electromagnetic CVT and electromagnetic seamless 2-speed gearbox and organic structural photo-capacitor for EV towards energy independent. He has published 140 index journal articles, 4 books and 8 patents.

Wajahat Khan obtained the bachelor of Engineering (Mechanical Engineering) from the NED University of Engineering and Technology (NEDUET), Pakistan, in 2018. He obtained a master of Engineering (Mechanical Engineering) from the NED University of Engineering and Technology (NEDUET), Pakistan, in 2022. He currently serves as a teaching faculty member at the National University of Sciences and Technology (NUST), PNEC Campus, Pakistan, since 2019. His research interests are composite materials, viscoelasticity, and Finite Element analysis.

Syed Mustafa Haider has been pursuing his doctoral degree in Manufacturing Engineering and Management from the Pakistan Navy Engineering College (PNEC), National University of Sciences and Technology (NUST), Pakistan, since 2022. He received his master's in Manufacturing Engineering from the University of Engineering and Technology (UET), Lahore, in 2019. His research interests are in the areas of machining and manufacturing technologies.